Journal of Autoimmunity

Research paper

Toll-like receptor 4 antagonist TAK-242 inhibits autoinflammatory symptoms in DITRA

Akitaka Shibata, M.D., Ph.D.[1,2], Kazumitsu Sugiura, M.D., Ph.D.[1,3], Yasuhide Furuta, Ph.D.[4], Yoshiko Mukumoto[4,5], Osamu Kaminuma, D.V.M., Ph.D.[6,7], and Masashi Akiyama M.D., Ph.D.[1,*]

[1]Department of Dermatology, Nagoya University Graduate School of Medicine, Nagoya, Japan.

[2]Department of Dermatology, Gifu Prefectural Tajimi Hospital, Tajimi, Japan

[3]Department of Dermatology, Fujita Health University School of Medicine, Toyoake, Japan

[4]Animal Resource Development Unit, RIKEN Center for Life Science Technologies, Kobe, Japan

[5]Genetic Engineering Team, RIKEN Center for Life Science Technologies, Kobe, Japan

[6]Department of Genome Medicine, Allergy and Immunology Project, Tokyo Metropolitan Institute of Medical Science, Tokyo, Japan

[7]The Center for Life Science Research, University of Yamanashi, Chuo, Japan

Subtitle

TAK242 inhibits DITRA autoinflammatory symptoms

Contents of manuscript

4614 words, 6 figures, 1 supplementary figure and 1 supplementary table.

*Corresponding author:

Dr. Masashi Akiyama, Department of Dermatology, Nagoya University Graduate School of Medicine, 65 Tsurumai-cho, Showa-ku, Nagoya, Aichi 466-8550, Japan (makiyama@med.nagoya-u.ac.jp)
Tel: +81-52-744-2314, Fax: +81-52-744-2318

ACKNOWLEDGMENTS

A.S. designed the study. A.S., K.S., and M.A. performed the experiments and analyzed the data. Y.F. and Y.M. generated the *Il36rn* knockout mice. O.K. performed flow cytometric analysis. A.S., K.S. and M.A. wrote the manuscript. All authors reviewed the final version of the manuscript.

This study was supported in part by JSPS KAKENHI grants 15H04887 (to M.A.), 15K15415 (to M.A.), 15H04886 (to K.S.), and 15K15414 (to K.S.); Technology of Japan Grant H26-itaku (nan)-ippan-027 to K.S. from the Japan Agency for Medical Research and Development, AMED (Practical Research Project for Rare / Intractable Diseases), Japan; the 7th Rohto Dermatology Prize (to K.S.) and by the Grant-in-Aid from the Japanese

Association of Geriatric Dermatology Research, 2015 (to K.S.).

This study was also supported in part by a Grant-in-Aid for Japanese Dermatological Association Basic Medicine Research Funds (contributed by the Shiseido Group) to A.S.

Funding sources had no involvement.

Conflicts of interest:

The authors declare no conflicts of interest.

Abstract

Background: *IL36RN* encodes the IL-36 receptor antagonist (IL-36Ra), and loss-of-function mutations in *IL36RN* define a recessively inherited autoinflammatory disease named "deficiency of IL-36Ra" (DITRA). DITRA causes systemic autoinflammatory diseases, including generalized pustular psoriasis (GPP), an occasionally life-threatening disease that is characterized by widespread sterile pustules on the skin, fever and other systemic symptoms. GPP can present at any age, and provocative factors include various infections, medicines and pregnancy.

Objective: We aimed to elucidate the role of toll-like receptor 4 (TLR4) signaling in DITRA and to innovate an efficient treatment for DITRA.

Methods: We generated *Il36rn*$^{-/-}$ mice and treated them with TLR4 agonist to establish DITRA model mice. Furthermore, we administrated TLR4 antagonist TAK-242 to the model mice to inhibit the DITRA symptoms.

Result: *Il36rn*$^{-/-}$ mice treated by TLR4 agonist showed autoinflammatory symptoms in skin, articulation and liver. Thus, we established model mice for DITRA or GPP that show cutaneous, articular, and hepatic autoinflammatory symptoms typical of DITRA or GPP: sterile pustules on the skin, liver abscesses and enthesitis of the hind paws. Additionally, these symptoms were canceled by TAK-242 administration. We demonstrated the inhibitory effects of the TLR4 antagonist TAK-242 on the autoinflammatory symptoms exhibited by the DITRA models.

Conclusion: We suggested that blockage of TLR4 signaling is a promising treatment for DITRA and GPP.

Key Words

autoinflammation, deficiency of IL-36 receptor antagonist, generalized pustular psoriasis, toll-like receptor 4, LPS, TAK-242

1 Introduction

IL36RN, also known as *IL1F5,* encodes the IL-36 receptor antagonist (IL-36Ra), which is an antagonist of IL-1-family cytokines. Loss-of-function mutations in *IL36RN* define a recessively inherited autoinflammatory disease named "deficiency of IL-36Ra" (DITRA) [1]. DITRA was first described in a subgroup of patients with generalized pustular psoriasis (GPP) [1, 2], which is a life-threatening disorder characterized by recurrent episodes of severe skin inflammation, with pustule development associated with fever, malaise, and extracutaneous involvement, including arthritis and neutrophilic cholangitis [2-4]. GPP skin lesions present recurrent sterile pustules with flush on the whole body. Psoriasis vulgaris (PV) exhibits multiple, hyperkeratotic erythematous plaques with scales. PV and GPP are variants of "psoriasis" which is an inflammatory skin disease with accelerated turnover of the epidermal keratinocytes. We reported that the majority of GPP without PV cases in Japanese are caused by mutations in *IL36RN* [2]. *IL36RN* mutations are thought to be a major predisposing factor for GPP, although certain triggering stimuli, such as TLR4 agonist activation, are probably needed for the onset of GPP. IL-36Ra is an IL-1 family cytokine, is an antagonist of the IL-36 receptor (IL-36R; also named IL-1RRP2 or IL-1RL2) and inhibits the activity of IL-36α, IL-36β, and IL-36γ (originally named IL-1F6, IL-1F8, and IL-1F9, respectively), which are also members of the IL-1 family of cytokines and are IL-36R agonists [5-9]. IL-1 is a major mediator of inflammation and exerts effects on the neuro-immuno-endocrine system. The IL-1 system is composed of the two agonist ligands IL-1α and IL-1β [10]. IL-1β is known to be derived from neutrophils and macrophages [11]. These cytokines activate several proinflammatory signaling pathways, such

as the nucleolar factor-κB and mitogen-activated protein-kinase pathways, which play important roles in innate immunity [12, 13]. Recently, IL-36 cytokines have attracted much attention for their important role in the initiation of psoriasis [1, 14].

In the past few years, a murine model of PV was generated by activation of TLR7, which recognizes viral single-stranded RNA [15, 16]. *Il36rn*$^{-/-}$ mice that were administered with a TLR7 agonist displayed more severe phenotypes associated with psoriasis vulgaris [17]. Although these models successfully reproduce the simple, acute skin inflammation of PV, they only partially reproduce the symptoms of DITRA. Concerning other TLRs, recent findings have indicated the importance of TLR4 and persistent inflammation in the development of obesity [18]. Moreover, Ballak *et al.* [19] reported that in obese mice, TLR4-signaling activation was attenuated by IL-37, which is an antagonist of IL-1-family cytokines. Therefore, we focused on the role of TLR4 instead of TLR7 in the onset of autoinflammatory reactions associated with DITRA. In this study, we established a model of autoinflammatory syndromes associated with DITRA via TLR4 activation in *Il36rn*$^{-/-}$ mice and successfully inhibited the onset of DITRA-related symptoms by using a selective TLR4 antagonist.

2 Methods

2.1 Mice. *Il36rn*$^{+/-}$ mice (Accession No. CDB1242K: http://www2.clst.riken.jp/arg/mutant%20mice%20list.html) were generated using a targeting vector designed to eliminate a part of exon 1 through the entire exon 3 by homologous recombination (Fig. 1a). A C57BL/6N embryonic stem cell line, HK3i [20], was transfected with the targeting vector by electroporation. We obtained F1 heterozygous mice by mating them to wild-type mice. Then, we intercrossed *Il36rn*$^{+/-}$ mice to generate *Il36rn*$^{-/-}$ mice. Males at 8–12 weeks were included in the experiment, and no randomization or blinding was used. Genotypes of the mice were determined by PCR analysis of the tail tissue DNA using the following primers: P1 (5'-ATGCATCCAAAGGCAGGTAA), P2 (5'-GCTTGGCTGGACGTAAACTC), P3 (5'-TGGAGCTCATGATGGTTCTG) and P4 (5'-AGGATCCTGCTCAGTTCTTCC). Primer sets P1-2 and P3-4 correspond to knockout allele 293bp and WT allele 205bp (Fig. 1b).

2.2 Antibodies, receptor agonists, and antagonists

Antibodies, receptor agonists, and antagonists used in this study for *in vivo* treatment were as follows: anti-mouse IL-17a antibody (catalog number: 16-7173-85; eBioscience, San Diego, CA, USA), mouse IgG1 K-isotype control functional grade purified antibody (catalog number: 16-4714-85; Biolegend, San Diego, CA, USA), TLR4 agonist lipopolysaccharide (LPS; catalog number: L3024; Sigma-Aldrich, St. Louis, MO, USA), TLR4 antagonist TAK-242 (catalog number: CS-0408; Chemscene, Monmouth Junction, NJ, USA), and CXCR2 antagonist SB225002 (catalog number: 13336; Cayman Chemical, Ann Arbor, MI, USA).

2.3 Hair removal from the back skin

The back skin of male WT mice or *Il36rn*$^{-/-}$ mice at 8–12 weeks of age was shaved with an electric clipper using depilatory cream (Epilat Kracie Sensitive Skin Hair Removal Cream; Kracie, Tokyo, Japan) 6 days prior to treatment.

2.4 Establishment of an imiquimod (IMQ)-induced psoriasis model

WT and *Il36rn*$^{-/-}$ mice were treated with topical application of commercially available 5% IMQ cream (Beselna Cream; kindly gifted by Mochida Pharmaceutical, Tokyo, Japan) at 62.5 mg IMQ per day for 5 consecutive days (from Days 1 to 5; the first IMQ application was done on Day 1; Fig. 2a). *Il36rn*$^{-/-}$ mice were treated with intraperitoneal injection of 5 mg/kg of the anti-IL-17a antibody or the control antibody on Day 0, or 3 mg/kg of the CXCR2 antagonist daily from Days 0 to 4 (Fig. 2a). Six hours after IMQ administration on Day 2, the mice were anesthetized and tissue samples from the back skin were collected for qualitative real-time PCR (qRT-PCR). On Day 6, the mice were anesthetized, and tissue samples from the back skin were collected for histopathologic and immunohistochemical (IHC) observation (Fig. 2a).

2.5 LPS-induced skin lesions and liver abscesses associated with deficiency of IL-36 receptor antagonist (DITRA) mice and inhibition by TLR4 antagonist

The mice received subcutaneous injection of LPS [3 μg dissolved in 50 μL distilled water (DW)] (50 μl) in the back skin once daily (Fig. 3a). *Il36rn*$^{-/-}$

mice were treated with intraperitoneal injection of 5 mg/kg TAK-242 or vehicle [dimethyl sulfoxide (DMSO) solution] from Days 0 to 2. TAK-242 dissolved in DMSO (10 mg/mL) was diluted in DW. The *Il36rn*$^{-/-}$ mice were also treated with the intraperitoneal injection of the anti-IL-17a antibody or the control antibody (5 mg/kg on Day 0) or 3 mg/kg of the CXCR2 antagonist daily from Days 0 to 2. On Day 2, the mice were anesthetized, and skin-tissue samples were collected from the back for qRT-PCR and enzyme-linked immunosorbent assay (ELISA) 4 h after LPS injection. At 4 h after LPS administration on Day 2, mice were anesthetized and tissue samples from the back skin and the liver were collected for qRT-PCR and ELISA. On Day 3, mice were anesthetized, and tissue samples of the back skin and liver were collected for qRT-PCR, histopathological observation, and IHC analysis. Inguinal lymph nodes were also collected for fluorescence-activated cell sorting (FACS) analysis on Day 3 (Fig. 3a). The areas of erythema and those of abscess/edema in the LPS-injected sites (2×2 cm square) were independently scored using four-point scoring systems from 0 to 3. Areas of erythema were scored as 0, none; 1, less than 25%; 2, 25% to 75%; 3, above 75%. Areas of abscess/edema were scored as 0, none; 1, less than 10%; 2, 10% to 50%; 3, above 50%. The severity indices of skin lesions were evaluated as the sum of both scores.

2.6 LPS-induced enthesitis associated with DITRA, and prevention by TLR4 antagonist

Mice received an intraplantar injection (e.g., into the subcutaneous tissue of the plantar surface of the paw) of LPS (300 ng/paw) or DW daily for 3 days (Fig. 6b). *Il36rn*$^{-/-}$ and WT mice were treated with an intraperitoneal

injection of 5 mg/kg TAK242 or vehicle (DMSO solution) from Days 0 to 3. At 6 h after the final injection on Day 3, the thickness of the hind paw was measured by micrometer (Quick-Mini; Mitsutoyo Corp., Kawasaki, Japan), and hind-paw tissue samples were collected for qRT-PCR and histopathological analysis (Fig. 6b).

2.7 Measurement of cytokine levels

Cytokine concentrations in the back skin, liver and hind paw were measured by ELISA. Three samples of 3-mm-thick punch biopsies were obtained from the back skin of mice and were flash-frozen in liquid nitrogen. The biopsy tissue fragments were homogenized in 400 μL phosphate-buffered saline (PBS) with Complete Protease Inhibitor Tablets (Roche, Basel, Switzerland) by a rotor homogenizer (Tissue Lyser LT; Qiagen, Hilden, Germany) and shaken in the solution at 4°C for 4 h. The supernatant was collected after centrifugation at 12,000 *g* for 5 min at 4°C. Total protein concentrations were measured by ultraviolet absorption spectrometry (NanoVue Plus; GE Healthcare, Tokyo, Japan). The concentrations of CXCL1, CXCL13, IL-1β and IL-17 in 10 μg total protein from skin tissue samples per single well were measured by commercially available ELISA kits according to the manufacturer's protocol (Duo Set, R&D Systems. Minneapolis, MN, USA).

2.8 Extraction of total RNA and qRT-PCR

We isolated total RNA from the back-skin and hind-paw tissue samples using the RNeasy Fibrous Tissue Mini Kit (Qiagen) and from the liver-tissue samples using the RNeasy Mini Kit (Qiagen). We reverse-transcribed 250 ng total RNA using the Prime Script RT Reagent Kit

(Takara, Shiga, Japan) according to manufacturer instructions, and the recovered cDNA was diluted 10-fold with DW for qRT-PCR. mRNA expression levels were measured by qRT-PCR using the Light Cycler System (Roche). The PCRs were set up in microcapillary tubes in a 10-μL reaction consisting of 2.5 μL of diluted cDNA solution, and the PCR program was set according to the manufacturer's instructions. Primers and probes used for qRT-PCR are listed in Supplementary Table 1.

2.9 Histopathological observations and IHC

Samples from the back skin, liver, and hind paw were fixed in 4% paraformaldehyde and embedded in paraffin. Tissue sections were deparaffinized and stained with hematoxylin and eosin (H&E). IHC was performed using the Vectastain ABC peroxidase kit (Vector Laboratories, Burlingame, CA, USA) as described previously[21], with slight modifications. Briefly, thin sections (4 μm) were cut from samples embedded in paraffin blocks and immersed in 0.01 M citric acid buffer containing 1 mM ethylenediaminetetraacetic acid for 5 min at 98°C for anti-TLR4 antibody staining, or immersed in 20 μg/mL proteinase K for 3 min at room temperature for anti-macrophage antibody staining. After the endogenous peroxidase activity was blocked with 0.3 % H_2O_2/methanol, the sections were incubated for 30 min in PBS with 4% bovine serum albumin (BSA) for blocking, followed by incubation overnight at 4°C with a primary rat anti-mouse F4/80 (clone A3-1) monoclonal antibody (catalog number: MCA497; Bio-Rad, Hercules, CA, USA) diluted to 1:100 or a primary rabbit anti-mouse TLR4 antibody (catalog number: Ab47093; Abcam, Cambridge, UK) diluted to 1:50. Sections were then incubated with biotin-conjugated goat anti-rat IgG antibody or goat anti-rabbit IgG

antibody for 60 min at room temperature and visualized according to the manufacturer's protocol.

2.10 Flow cytometric analysis. After blocking with Fc Block (BD Bioscience) in PBS containing 3% BSA, inguinal lymph node cells were stained with anti-mouse γδTCR-APC antibody (catalog number: 17-5711; eBioscience), anti-mouse TCRβ-PE antibody (catalog number: 12-5961; eBioscience), anti-mouse Gr-1-APC-eFluor780 antibody (catalog number: 47-5931; eBioscience), anti-mouse CD3-PECy7 (catalog number: 552774; BD Bioscience), anti-mouse CD19-PE antibody (clone 1D3; BD Bioscience), anti-mouse Siglec-F-PE antibody (clone E50-2440; BD Bioscience), anti-mouse CD11b-PerCP-Cy5.5 (clone M1/70; BD Bioscience), anti-CD11c-biotin antibody (clone HL3; BD Bioscience) plus streptavidin-Pacific Blue (catalog number: S11222; Invitrogen), and/or αGarCer-CD1d-APC (catalog number: E001-4; Proimmune). Flow cytometric analysis was performed using a BD FACS Canto II workstation (BD Bioscience) with FlowJo data analysis software (FLOWJO, LLC) as described previously [22]. $CD3^-CD19^+$, $CD3^+CD19^-$, $CD3^+\gamma\delta TCR^+$, $TCR\beta^+\alpha$-GarCer/$CD1d^+$, $CD11c^+$Siglec-F^-, $CD11c^-$Siglec-F^+, $CD11b^{high}Gr\text{-}1^{high}$, and $CD11b^{low}Gr\text{-}1^-$ cells were indicators of B cells, T cells, γδT cells, natural killer (NK) T cells, dendritic cells, eosinophils, neutrophils, and macrophages, respectively.

2.11 Skin-permeability assay

Transepidermal water loss (TEWL) was measured on live mice by evaporimeter (AS-VT100RS; Asahibiomed Corp, Tokyo, Japan). The AS-VE-100RS utilizes the ventilated-chamber method for measuring TEWL,

and TEWL measurements were performed on the backs of the mice at the skin biopsy sites immediately before biopsy.

2.12 Statistical analyses

Data of qRT-PCR, ELISA, flow cytometric analysis, skin-permeability assay and measurements of skin erythema areas, abscess/edema areas and hind-paw thickness were presented as mean±SD and analyzed by one-way Student's *t* test. Significant differences were shown as ***$P<0.001$, **$P<0.01$, *$P<0.05$.

2.13 Study approval

All studies and procedures were approved by the Committee on Animal Experimentation of Nagoya University and RIKEN Kobe.

3 Results

3.1 IMQ-induced psoriatic skin inflammation in *Il-36rn*$^{-/-}$ mice

We generated *Il36rn*$^{-/-}$ mice (see additional information in the Methods section in this article's Online Repository) (Fig. 1a, b). We observed several *Il36rn*$^{-/-}$ and *Il36rn*$^{+/-}$ mice for 1 year and dissected them, but no spontaneous psoriasiform dermatitis nor liver abscesses were present. Thus, we established IMQ-induced psoriasiform dermatitis in *Il36rn*$^{-/-}$ mice by topical application of IMQ to the back skin (see additional information in the Methods section in this article's Online Repository) (Fig. 2a). The *Il36rn*$^{-/-}$ mice showed manifestations of psoriasis, such as scaling, erythema, and thickening of the skin, that were more severe than the manifestations shown by WT mice (Fig. 2b). Consistent with clinical features, H&E-stained sections of IMQ-treated *Il36rn*$^{-/-}$ mouse skin demonstrated acanthosis, parakeratosis, and disturbed keratinocyte differentiation that were more severe than those in IMQ-treated WT mouse skin (Fig. 2b). These results were in agreement with those of previous studies [17, 23].

We then treated IMQ-induced psoriasis model *Il36rn*$^{-/-}$ mice with the anti-IL-17a antibody and the CXCR2 antagonist to elucidate the cytokines responsible for neutrophil recruitment (Fig. 2a). IL-17a is a Th-17 cytokine, and mice do not have an ortholog of human IL-8. However, mouse neutrophils express a receptor homologous to human CXCR2 that mediates neutrophil chemotaxis in response to human IL-8 and whose ligands are CXCL1 and CXCL2 [24, 25]. The anti-IL-17a antibody and the CXCR2 antagonist attenuated the clinical symptoms to some extent (Fig. 2b), and the anti-IL-17a antibody significantly diminished skin-barrier disruption as measured by transepidermal water loss (TEWL) (Fig. 2c). Consistent with the diminution of clinical symptoms, histological features

were attenuated significantly in *Il36rn*$^{-/-}$ mice treated with the anti-IL-17a antibody and the CXCR2 antagonist (Fig. 2b).

Cxcl1 and *Il36a* mRNA levels measured with quantitative real-time polymerase chain reaction (qRT-PCR) were significantly elevated in the skin of IMQ-treated WT and *Il36rn*$^{-/-}$ mice (Fig. 2d), while *Il1b*, *Cxcl2*, *Il17a*, and *Tnf* mRNA levels were elevated, though not significantly, in the skin of IMQ-treated WT and *Il36rn*$^{-/-}$ mice. *Cxcl1, Cxcl2*, *Il1b,* and *Il17a* mRNA expression levels decreased in *Il36rn*$^{-/-}$ mice treated with the anti-IL-17a antibody and the CXCR2 antagonist (Fig. 2d). Collectively, these results suggest that the CXCL1 and IL-17a pathways play an important role in IMQ-induced psoriasis in *Il36rn*$^{-/-}$ mice. However, the IMQ-induced skin manifestations in *Il36rn*$^{-/-}$ mice only partially reproduced the symptoms of DITRA; they did not reproduce the pustular lesions. We thought that this model presented PV skin lesions, but not DITRA or GPP skin lesions. Thus, we tried activation of another TLR pathway, TLR4, described in Section 2.5.

3.2 LPS-induced skin lesions associated with DITRA in *Il36rn*$^{-/-}$ mice

From our abovementioned thought that the activated TLR4-signaling pathway is associated with continuous inflammation in *Il36rn*$^{-/-}$ and *Il36rn*$^{+/-}$ mice, we addressed the role of the TLR4 pathway in pathomechanisms of DITRA. Lipopolysaccharide (LPS), a structural component of the outer membrane of Gram-negative bacteria, is recognized by TLR4 and initiates downstream signaling via MyD88, TIRAP/Mal, IL-1R-associated kinases 1, 2, and 4, and TNFR-associated factor-6 [26, 27]. Additionally, TLR4 activation leads to the initiation of a proinflammatory

cascade [28]. We established an LPS-induced model of pustular skin lesions associated with DITRA in *Il36rn*$^{-/-}$ mice by subcutaneous injection of LPS (Fig. 3a). *Il36rn*$^{-/-}$ mice receiving subcutaneous injection of LPS (3 μg) revealed severe skin abscesses and erythemas, while similarly treated WT mice showed only mild erythematous lesions and slight abscesses (Fig. 3b, c and Fig. S1). Consistent with the clinical features, H&E-stained sections of the LPS-treated *Il36rn*$^{-/-}$ mouse skin demonstrated neutrophilic infiltration and hemorrhage in the dermis that were more prominent than those of LPS-treated WT mice (Fig. 3b). LPS-treated WT and *Il36rn*$^{-/-}$ mice demonstrated macrophage infiltration in the dermis (Fig. 3b), whereas LPS-treated *Il36rn*$^{-/-}$ mice demonstrated elevated TLR4 expression in the dermis as compared with LPS-treated WT mice (Fig. 3b). *Cxcl1* and *Il6* mRNA were more greatly elevated in the skin of LPS-treated *Il36rn*$^{-/-}$ mice than in the skin of LPS-treated WT mice on Day 2 (Fig. 3e), and *Tnf*, *Il1b*, *Il36a*, and *Il36g* mRNA were elevated in the skin of both the LPS-treated *Il36rn*$^{-/-}$ mice and the LPS-treated WT mice on Day 2 (Fig. 3e), although *Il17a* mRNA levels never increased (data not shown). CXCL1, CXCL13, and IL-1β cytokine levels as detected by enzyme-linked immunosorbent assay (ELISA) were more elevated in the skin of LPS-treated *Il36rn*$^{-/-}$ mice than in LPS-treated WT mice on Day 2 (Fig. 3f). However, IL-17a concentrations did not increase in LPS-treated *Il36rn*$^{-/-}$ or WT mice (Fig. 3f). These findings indicate that LPS-induced DITRA-related skin lesions were established in *Il36rn*$^{-/-}$ mice by TLR4 pathway activation.

3.3 LPS-induced liver abscesses in *Il36rn*$^{-/-}$ mice

LPS-induced *Il36rn*$^{-/-}$ DITRA mice exhibited both skin and hepatic lesions. LPS-induced *Il36rn*$^{-/-}$ mice with pustular skin lesions associated with

DITRA also exhibited focal liver abscesses, whereas LPS-treated WT mice did not exhibit liver abscesses (Fig. 4a, b). Consistent with the clinical features, H&E-stained sections of the liver from LPS-treated *Il36rn*$^{-/-}$ mice demonstrated focal abscesses with neutrophilic infiltration and neutrophilic cholangitis in the liver. The abscess areas were surrounded by macrophage infiltration (Fig. 4a). *Cxcl1* mRNA levels were more significantly elevated in the livers of LPS-treated *Il36rn*$^{-/-}$ mice than in those of LPS-treated WT mice on Day 3 (Fig. 4d). Additionally, *Il1b*, Il6, *Tnf* and *Il36g* mRNA levels were elevated in the livers of both LPS-treated *Il36rn*$^{-/-}$ and WT mice, but without significant differences on Day 2 (Fig. 4d). *Il17, Il36a and Il36b* mRNA expression was not detected in the livers of either LPS-treated *Il36rn*$^{-/-}$ or WT mice (data not shown). These findings indicate that the LPS-induced *Il36rn*$^{-/-}$ DITRA mice exhibited hepatic abscesses via CXCL1 signaling.

3.4 Flow cytometric analysis of inguinal lymph node cells

We then performed flow cytometric analysis of inguinal lymph node cells to clarify whether LPS administration to the skin evoked a systemic immune reaction. The B cell counts significantly were significantly elevated in the lymph nodes of LPS-treated *Il36rn*$^{-/-}$ mice compared with those of control non-LPS-treated *Il36rn*$^{-/-}$ mice or LPS-treated WT mice (Fig. 5a). The γδ cell count increased slightly in both LPS-treated WT and *Il36rn*$^{-/-}$ mice (Fig. 5b). However, macrophages, natural killer T cells, dendritic cells, eosinophils and neutrophils did not increase in either the LPS-treated WT or *Il36rn*$^{-/-}$ mice (Fig. 5c, d, e).

3.5 LPS-induced enthesitis associated with DITRA in *Il36rn*$^{-/-}$ mice

We discovered spontaneous arthritis in *Il36rn*$^{+/-}$ and *Il36rn*$^{-/-}$ mice that was likely induced by continual insult and minor injuries (Fig. 6a). Therefore, our assessment was that continual insult and infection trigger DITRA-related arthritis (enthesitis) in *Il36rn*$^{+/-}$ and *Il36rn*$^{-/-}$ mice. We then investigated the development of LPS-induced DITRA-related enthesitis in *Il36rn*$^{-/-}$ mice by intraplantar LPS injection (Fig. 6b). The hind paws of *Il36rn*$^{-/-}$ mice that had received 300 ng LPS were significantly thicker than those of WT mice (Fig. 6c, d). H&E-stained sections from the hind paws of LPS-treated *Il36rn*$^{-/-}$ mice demonstrated more prominent neutrophilic infiltration than in those of LPS-treated WT mice (Fig. 6c). We also detected increased levels of *Cxcl1, Il6, Il1b*, *Tnf,* and *Il36g* mRNA in the hind paws of both LPS-treated *Il36rn*$^{-/-}$ and WT mice (Fig. 6e). These findings indicate that LPS-induced DITRA-related enthesitis was established in *Il36rn*$^{-/-}$ mice via TLR4-pathway activation predominantly through CXCL1, IL-6, TNF, and IL-36γ signaling.

3.6 Blockade of the TLR4 pathway prevents skin lesions associated with DITRA in *Il36rn*$^{-/-}$ mice

TAK-242 (resatorvid; catalog number: CS-0408; Chemscene, Monmouth Junction, NJ, USA) was synthesized by Takeda Pharmaceutical Co., Ltd. (Osaka, Japan). It is a small-molecule-specific inhibitor of TLR4 signaling that inhibits the production of LPS-induced inflammatory mediators by binding to the intracellular domain of TLR4 [29, 30]. The wild-type mice developed almost no symptoms of DITRA or GPP. Thus, we did not administer TAK-242 to the wild-type mice. Daily pretreatment of *Il36rn*$^{-/-}$ mice with the TLR4 antagonist TAK-242 from Days 0 to 2 blocked LPS-

induced pustular skin formation in *Il36rn*$^{-/-}$ mice that had received 3 μg of LPS (Fig. 3a, b, c). Consistent with the improved clinical features, H&E-stained sections of skin samples from these mice demonstrated neither neutrophilic infiltration nor hemorrhage in the dermis (Fig. 3b). The increases in *Cxcl1 and Il6* mRNA levels in the skin of LPS-treated *Il36rn*$^{-/-}$ mice were also alleviated by TAK-242 administration, although increased mRNA expression of *Il1b*, *Tnf, Il36a*, or *Il36g* was not altered by TAK-242 treatment (Fig. 3e). Additionally, increased concentrations of IL-1b, CXCL1, and CXCL13 detected by ELISA in the skin of LPS-treated *Il36rn*$^{-/-}$ mice were attenuated by TAK-242 administration (Fig. 3f). IL-17a concentrations did not increase in the *Il36rn*$^{-/-}$ mice nor in the WT mice (Fig. 3f). The *Il36rn*$^{-/-}$ mice were also treated with intraperitoneal injection of anti-IL-17a antibody or the CXCR2 antagonist; however, these treatments did not diminish the skin manifestations (Fig. 3d). These findings indicate that LPS-induced skin lesions associated with DITRA were attenuated by blockage of the TLR4-signaling pathway, but not by treatment with the anti-IL-17a antibody or the CXCR2 antagonist.

3.7 Blockage of the TLR4-signaling pathway inhibits the formation of LPS-induced liver abscesses associated with DITRA

LPS-treated *Il36rn*$^{-/-}$ mice administered with TAK-242 only rarely showed abscesses (Fig 4a, b). Elevated expression of *Cxcl1* mRNA in the liver was attenuated by TAK-242 administration (Fig. 4d). Similarly, increases in *Il1b*, *Il6*, *and Tnf* mRNA expression in the liver were also attenuated by TAK-242 treatment (Fig. 4d). The DITRA mice were also treated with intraperitoneal injection of anti-IL-17a antibodies or a CXCR2 antagonist, with minimal effect on the liver abscesses (Fig. 4c). These findings indicate

that LPS-induced lesions in the liver associated with DITRA were alleviated by blockage of the TLR4-signaling pathway.

3.8 Blockage of the TLR4-signaling pathway prevents LPS-induced enthesitis associated with DITRA in *Il36rn*$^{-/-}$ mice

We treated LPS-induced DITRA *Il36rn*$^{-/-}$ mice presenting with enthesitis by intraperitoneal injection of TAK-242 (5 mg/kg/day) from Days 0 to 3 (Fig. 6b). The *Il36rn*$^{-/-}$ mice that had received 300 ng LPS and were treated with TAK-242 exhibited diminished thickening of the hind paw (Fig. 6c, d). Additionally, neutrophilic infiltration was attenuated in the LPS-treated *Il-36rn*$^{-/-}$ mice administered with TAK-242 (Fig. 6c). Increased *Cxcl1, Il1b*, and *Il6* and *Tnf* mRNA levels in the hind paws of LPS-treated *Il36rn*$^{-/-}$ mice were also alleviated by TAK-242 pretreatment (Fig. 6e). However, increased *Il36a*, or *Il36g* mRNA levels in the hind paws of LPS-treated *Il36rn*$^{-/-}$ mice were not prevented by pretreatment of TAK-242 (Fig. 6e). These findings indicate that LPS-induced DITRA-related enthesitis was prevented by blockage of the TLR4-signaling pathway.

4 Discussion

IL36RN encodes IL-36Ra, and loss-of-function mutations with autosomal recessive inheritance in *IL36RN* define a recessively inherited autoinflammatory disease named DITRA[1]. DITRA is a life-threatening disorder characterized by recurrent episodes of severe skin inflammation, with pustule development associated with fever, malaise, and extracutaneous involvement, including arthritis and neutrophilic cholangitis. The relation between DITRA and arthritis has not been elucidated so far [31].Recently, IL-36 cytokines have gained attention due to their important role in the initiation of psoriasis [1, 14]. Moreover, Th17 cytokines have been elucidated as the mechanism of PV [32-34].

IL-36 cytokines have been reported to be involved in the development of psoriasis in an Il-36rn mice model stimulated by IMQ [1]. IMQ invokes the Th17 pathway via the TLR7 receptor co-associated with Il-1b [23]. Furthermore, the Il-36α-deficient mice treated with IMQ did not develop psoriasiform dermatitis, whereas the Il-36β-deficient mice and Il-36γ-deficient mice did develop psoriasiform dermatitis [23]. Il-36α and Il-36R signaling is thought to be essential for the development of IMQ-induced psoriasis model lesions via crosstalk between dendritic cells and keratinocytes. However, the present study only addresses partial DITRA skin manifestations via the TLR7 pathway.

Concerning other TLR pathways, the importance of TLR4 in several disorders of innate immunity such as inflammatory bowel diseases, adult respiratory distress syndromes, acute renal failure, inflammatory pain and a metabolic syndrome has been emphasized based on recent evidence [18, 35-42]. LPS is a glucolipid constituent of the outer membrane of Gram-negative bacteria [43] and is recognized by TLR4. TLR4 activation induces a signaling cascade via MyD88, TIRAP/Mal, IL-1R-associated kinases 1, 2,

and 4, and TNFR-associated factor-6 [26, 27], leading to the activation of NF-κB and the production of proinflammatory cytokines [28, 44].

Recently, an association between PV and metabolic syndromes has been shown [45]. Saturated fatty acids are recognized by TLR4 and induce the secretion of inflammatory cytokines such as TNF, leading to chronic inflammation both in PV and in metabolic syndromes [42].

GPP as a skin manifestation of DITRA is often triggered by infection in IL36RN-deficient individuals [2]. Thus, in the present study, we raise the possibility that TLR4 pathway activation by the TLR4 agonist leads to the manifestations shown by the DITRA skin model. In this model, we also tried to induce the systemic inflammation that is seen in PV and GPP patients.

In our DITRA skin model induced by LPS in *Il36rn*$^{-/-}$ mice, not only are the skin lesions reproduced, but so are the liver manifestations with neutrophilic infiltration and intrahepatic neutrophilic cholangitis. In the previously reported IMQ-induced psoriasis skin model in *Il36rn*$^{-/-}$ mice, the skin manifestations developed via crosstalk between dendritic cells and keratinocytes, and Il-36α was recognized as an important subset of Il-36 cytokines [23]. In our present DITRA model, the Il36Ra and TLR4 pathways work in coordination in the development of the DITRA skin model and subsequent systemic inflammation leading to liver abscesses. In the present liver lesions, IL-36γ increased but IL-36α did not (Fig. 5d). Thus, we assume that it is IL-36γ and not IL-36α that plays an important role in systemic inflammation in our model. From the qRT-PCR and ELISA analysis of the cutaneous and hepatic lesions, we think that Cxcl1, IL-6, IL-36α and IL-36γ play important roles as leading cytokines, rather than IL-17a playing such a role.

Psoriatic arthritis also occurs with PV [46]. TNF is thought to play important roles in the pathomechanism of psoriatic arthritis [47, 48]. In our DITRA enthesis model induced by LPS-treatment in *Il36rn*$^{-/-}$ mice, we clearly demonstrated by qRT-PCR analysis of the hind-paw lesions that Cxcl1, IL-1β, IL-6, TNF, and IL-36γ play important roles as leading cytokines in the pathogenesis of DITRA-associated arthritis.

The three major autoinflammatory symptoms of the DITRA model (skin abscesses, liver abscesses and hind-paw enthesitis) were successfully alleviated by TAK-242 treatment (Fig. 3b, 4a, 6c), which has proven safe for human use [49]. TAK-242 (also called resatorvid) is a small-molecule-specific inhibitor of TLR4 signaling, and it inhibits the production of LPS-induced inflammatory mediators by binding to the intracellular domain of TLR4 [29]. Increased protein concentrations and mRNA expression levels of cytokines, including CXCL1, CXCL13, and IL-1β, in the tissues of LPS-treated *Il36rn*$^{-/-}$ mice were abolished by TAK-242 administration (Fig. 3e, f, 4d, 6e). The DITRA mice were also treated with intraperitoneal injection of anti-IL-17a antibodies or a CXCR2 antagonist, with minimal effect on the skin and liver abscesses (Fig. 3d, 4c). From the present results, the blockade of the TLR4 pathway was proven to be a possible treatment not only for the skin lesions of DITRA, but also for the systemic inflammation of DITRA, including the liver manifestations.

Although the roles of TLR4 signaling in the development of DITRA inflammatory symptoms have not been completely elucidated, known DITRA-triggering factors, such as infection, medication, and pregnancy, may activate TLR4 signaling. Furthermore, serum CXCL1 levels have been found to increase in GPP patients, and that increase has been found to

correlate with their clinical severity [50]. The data presented here from our DITRA model are consistent with the previous reports.

5 Conclusion

Via TLR4-signaling activation, we established a model of the systemic autoinflammatory symptoms of DITRA: the cutaneous, hepatic, and articular lesions in *Il36rn*$^{-/-}$ mice. In addition, we showed that the TLR4 antagonist TAK-242 prevents all three symptoms. These data suggest that inhibition of TLR4 signaling constitutes a promising treatment strategy for autoinflammatory symptoms associated with DITRA.

References

[1] Marrakchi S, Guigue P, Renshaw BR, Puel A, Pei XY, Fraitag S *et al.* Interleukin-36-receptor antagonist deficiency and generalized pustular psoriasis. N Engl J Med, 2011;365**:**620-8.

[2] Sugiura K, Takemoto A, Yamaguchi M, Takahashi H, Shoda Y, Mitsuma T *et al.* The majority of generalized pustular psoriasis without psoriasis vulgaris is caused by deficiency of interleukin-36 receptor antagonist. J Invest Dermatol, 2013;133**:**2514-21.

[3] Sugiura K, Muto M, Akiyama M. CARD14 c.526G>C (p.Asp176His) is a significant risk factor for generalized pustular psoriasis with psoriasis vulgaris in the Japanese cohort. J Invest Dermatol, 2014;134**:**1755-7.

[4] Cabanillas M, Perez-Perez L, Sanchez-Aguilar D, Toribio J. [Generalized pustular psoriasis and cytolytic hepatitis associated with neutrophilic cholangitis]. Actas Dermosifiliogr, 2006;97**:**330-3.

[5] Kumar S, McDonnell PC, Lehr R, Tierney L, Tzimas MN, Griswold DE *et al.* Identification and initial characterization of four novel members of the interleukin-1 family. J Biol Chem, 2000;275**:**10308-14.

[6] Smith DE, Renshaw BR, Ketchem RR, Kubin M, Garka KE, Sims JE. Four new members expand the interleukin-1 superfamily. J Biol Chem, 2000;275**:**1169-75.

[7] Blumberg H, Dinh H, Dean C, Jr., Trueblood ES, Bailey K, Shows D *et al.* IL-1RL2 and its ligands contribute to the cytokine network in psoriasis. J Immunol, 2010;185**:**4354-62.

[8] Dinarello C, Arend W, Sims J, Smith D, Blumberg H, O'Neill L *et al.* IL-1 family nomenclature. Nat Immunol, 2010;11**:**973.

[9] Sims JE, Smith DE. The IL-1 family: regulators of immunity. Nat Rev Immunol, 2010;10**:**89-102.

[10] Dinarello CA. Interleukin-1, interleukin-1 receptors and interleukin-1 receptor antagonist. Int Rev Immunol, 1998;16**:**457-99.

[11] Sumida H, Yanagida K, Kita Y, Abe J, Matsushima K, Nakamura M *et al.* Interplay between CXCR2 and BLT1 facilitates neutrophil infiltration and resultant keratinocyte activation in a murine model of imiquimod-induced psoriasis. J Immunol, 2014;192**:**4361-9.

[12] Debets R, Timans JC, Homey B, Zurawski S, Sana TR, Lo S *et al.* Two novel IL-1 family members, IL-1 delta and IL-1 epsilon, function as an antagonist and agonist of NF-kappa B activation through the orphan IL-1 receptor-related protein 2. J Immunol, 2001;167**:**1440-6.

[13] Towne JE, Garka KE, Renshaw BR, Virca GD, Sims JE. Interleukin (IL)-1F6, IL-1F8, and IL-1F9 signal through IL-1Rrp2 and IL-1RAcP to activate the pathway leading to NF-kappaB and MAPKs. J Biol Chem, 2004;279**:**13677-88.

[14] Johnston A, Xing X, Guzman AM, Riblett M, Loyd CM, Ward NL *et al.* IL-1F5, -F6, -F8, and -F9: a novel IL-1 family signaling system that is active in psoriasis and promotes keratinocyte

antimicrobial peptide expression. J Immunol, 2011;186**:**2613-22.

[15] van der Fits L, Mourits S, Voerman JS, Kant M, Boon L, Laman JD *et al.* Imiquimod-induced psoriasis-like skin inflammation in mice is mediated via the IL-23/IL-17 axis. J Immunol, 2009;182**:**5836-45.

[16] Cai Y, Shen X, Ding C, Qi C, Li K, Li X *et al.* Pivotal role of dermal IL-17-producing gammadelta T cells in skin inflammation. Immunity, 2011;35**:**596-610.

[17] Tortola L, Rosenwald E, Abel B, Blumberg H, Schafer M, Coyle AJ *et al.* Psoriasiform dermatitis is driven by IL-36-mediated DC-keratinocyte crosstalk. J Clin Invest, 2012;122**:**3965-76.

[18] Konner AC, Bruning JC. Toll-like receptors: linking inflammation to metabolism. Trends Endocrinol Metab, 2011;22**:**16-23.

[19] Ballak DB, van Diepen JA, Moschen AR, Jansen HJ, Hijmans A, Groenhof GJ *et al.* IL-37 protects against obesity-induced inflammation and insulin resistance. Nat Commun, 2014;5**:**4711.

[20] Kiyonari H, Kaneko M, Abe S, Aizawa S. Three inhibitors of FGF receptor, ERK, and GSK3 establishes germline-competent embryonic stem cells of C57BL/6N mouse strain with high efficiency and stability. Genesis, 2010;48**:**317-27.

[21] Sugiura K, Muro Y, Nishizawa Y, Okamoto M, Shinohara T, Tomita Y *et al.* LEDGF/DFS70, a major autoantigen of atopic dermatitis, is a component of keratohyalin granules. J Invest Dermatol, 2007;127**:**75-80.

[22] Kaminuma O, Ohtomo T, Mori A, Nagakubo D, Hieshima K, Ohmachi Y *et al.* Selective down-regulation of Th2 cell-mediated airway inflammation in mice by pharmacological intervention of CCR4. Clin Exp Allergy, 2012;42**:**315-25.

[23] Milora KA, Fu H, Dubaz O, Jensen LE. Unprocessed Interleukin-36alpha Regulates Psoriasis-Like Skin Inflammation in Cooperation With Interleukin-1. J Invest Dermatol, 2015.

[24] Lee J, Cacalano G, Camerato T, Toy K, Moore MW, Wood WI. Chemokine binding and activities mediated by the mouse IL-8 receptor. J Immunol, 1995;155**:**2158-64.

[25] Bozic CR, Gerard NP, von Uexkull-Guldenband C, Kolakowski LF, Jr., Conklyn MJ, Breslow R *et al.* The murine interleukin 8 type B receptor homologue and its ligands. Expression and biological characterization. J Biol Chem, 1994;269**:**29355-8.

[26] Kawai T, Akira S. Toll-like receptors and their crosstalk with other innate receptors in infection and immunity. Immunity, 2011;34**:**637-50.

[27] Kumar H, Kawai T, Akira S. Toll-like receptors and innate immunity. Biochem Biophys Res Commun, 2009;388**:**621-5.

[28] Cappelletti C, Galbardi B, Kapetis D, Vattemi G, Guglielmi V, Tonin P *et al.* Autophagy, inflammation and innate immunity in inflammatory myopathies. PLoS One, 2014;9**:**e111490.

[29] Ii M, Matsunaga N, Hazeki K, Nakamura K, Takashima K, Seya T *et al.* A novel cyclohexene

derivative, ethyl (6R)-6-[N-(2-Chloro-4-fluorophenyl)sulfamoyl]cyclohex-1-ene-1-carboxylate (TAK-242), selectively inhibits toll-like receptor 4-mediated cytokine production through suppression of intracellular signaling. Mol Pharmacol, 2006;69**:**1288-95.

[30] Matsunaga N, Tsuchimori N, Matsumoto T, Ii M. TAK-242 (resatorvid), a small-molecule inhibitor of Toll-like receptor (TLR) 4 signaling, binds selectively to TLR4 and interferes with interactions between TLR4 and its adaptor molecules. Mol Pharmacol, 2011;79**:**34-41.

[31] Dietrich D, Gabay C. Inflammation: IL-36 has proinflammatory effects in skin but not in joints. Nat Rev Rheumatol, 2014;10**:**639-40.

[32] Lowes MA, Kikuchi T, Fuentes-Duculan J, Cardinale I, Zaba LC, Haider AS *et al.* Psoriasis vulgaris lesions contain discrete populations of Th1 and Th17 T cells. J Invest Dermatol, 2008;128**:**1207-11.

[33] Lowes MA, Bowcock AM, Krueger JG. Pathogenesis and therapy of psoriasis. Nature, 2007;445**:**866-73.

[34] Nickoloff BJ. Cracking the cytokine code in psoriasis. Nat Med, 2007;13**:**242-4.

[35] Oostenbrug LE, Drenth JP, de Jong DJ, Nolte IM, Oosterom E, van Dullemen HM *et al.* Association between Toll-like receptor 4 and inflammatory bowel disease. Inflamm Bowel Dis, 2005;11**:**567-75.

[36] Ramirez Cruz NE, Maldonado Bernal C, Cuevas Uriostegui ML, Castanon J, Lopez Macias C, Isibasi A. Toll-like receptors: dysregulation in vivo in patients with acute respiratory distress syndrome. Rev Alerg Mex, 2004;51**:**210-7.

[37] Heemann U, Szabo A, Hamar P, Muller V, Witzke O, Lutz J *et al.* Lipopolysaccharide pretreatment protects from renal ischemia/reperfusion injury : possible connection to an interleukin-6-dependent pathway. Am J Pathol, 2000;156**:**287-93.

[38] Calil IL, Zarpelon AC, Guerrero AT, Alves-Filho JC, Ferreira SH, Cunha FQ *et al.* Lipopolysaccharide induces inflammatory hyperalgesia triggering a TLR4/MyD88-dependent cytokine cascade in the mice paw. PLoS One, 2014;9**:**e90013.

[39] Pasternak BA, D'Mello S, Jurickova, II, Han X, Willson T, Flick L *et al.* Lipopolysaccharide exposure is linked to activation of the acute phase response and growth failure in pediatric Crohn's disease and murine colitis. Inflamm Bowel Dis, 2010;16**:**856-69.

[40] Mei SH, McCarter SD, Deng Y, Parker CH, Liles WC, Stewart DJ. Prevention of LPS-induced acute lung injury in mice by mesenchymal stem cells overexpressing angiopoietin 1. PLoS Med, 2007;4**:**e269.

[41] Wu H, Chen G, Wyburn KR, Yin J, Bertolino P, Eris JM *et al.* TLR4 activation mediates kidney ischemia/reperfusion injury. J Clin Invest, 2007;117**:**2847-59.

[42] Jin C, Flavell RA. Innate sensors of pathogen and stress: linking inflammation to obesity. J Allergy Clin Immunol, 2013;132**:**287-94.

[43] Freudenberg MA, Galanos C. Bacterial lipopolysaccharides: structure, metabolism and mechanisms of action. Int Rev Immunol, 1990;6**:**207-21.

[44] Shimazu R, Akashi S, Ogata H, Nagai Y, Fukudome K, Miyake K *et al.* MD-2, a molecule that confers lipopolysaccharide responsiveness on Toll-like receptor 4. J Exp Med, 1999;189**:**1777-82.

[45] Armstrong AW, Harskamp CT, Armstrong EJ. Psoriasis and metabolic syndrome: a systematic review and meta-analysis of observational studies. J Am Acad Dermatol, 2013;68**:**654-62.

[46] Yamamoto T. Psoriatic arthritis: from a dermatological perspective. Eur J Dermatol, 2011;21**:**660-6.

[47] Barnas JL, Ritchlin CT. Etiology and Pathogenesis of Psoriatic Arthritis. Rheum Dis Clin North Am, 2015;41**:**643-63.

[48] de Vlam K, Gottlieb AB, Mease PJ. Current concepts in psoriatic arthritis: pathogenesis and management. Acta Derm Venereol, 2014;94**:**627-34.

[49] Rice TW, Wheeler AP, Bernard GR, Vincent JL, Angus DC, Aikawa N *et al.* A randomized, double-blind, placebo-controlled trial of TAK-242 for the treatment of severe sepsis. Crit Care Med, 2010;38**:**1685-94.

[50] Kato Y, Yamamoto T. Increased serum levels of growth-related oncogene-alpha in patients with generalized pustular psoriasis. Dermatology, 2010;220**:**46-8.

Figure legends

Figure 1 Establishment of the IL-36Ra deficient obese mice

(**a**) The targeting vector was constructed by disrupting exon 1 through the entire exon 3. (**b**) PCR reaction amplified a 293-bp mutant band, and a 205-bp fragment corresponding to the wild-type (WT) genomic *Il36rn* DNA.
(**c**) Aged *Il36rn*$^{-/-}$ and *Il36rn*$^{+/-}$ mice (44-week-old) presented with obesity.
(**d**) The body weight of wild-type (WT) (n=11), *Il36rn*$^{+/-}$ (n=9), and *Il36rn*$^{-/-}$ (n=7). The body weights of both *Il36rn*$^{+/-}$ and *Il36rn*$^{-/-}$ mice are significantly greater than those of WT mice at 44 weeks of age. Error bars represent mean±SD. *$p < 0.05$, data analyzed by unpaired one-way t test.
(**e**) Plasma insulin levels of WT (n=8; left panel), *Il36rn*$^{-/-}$ (n=7; middle panel), and *Il36rn*$^{+/-}$ (n=9; left panel) mice at 44 weeks of age. Plasma insulin levels are positively associated with body weights in *Il36rn*$^{+/-}$ and *Il36rn*$^{-/-}$ mice, but not in WT or *Il36rn*$^{-/-}$ mice.

Figure 2 IMQ-induced psoriasis vulgaris model in *Il36rn*$^{-/-}$ mice

(**a**) Protocols for the development of an imiquimod (IMQ)-induced psoriasis model. Wild-type (WT) and *Il36rn*$^{-/-}$ (KO) mice were treated with topical application of IMQ for 5 consecutive days (from Day 1 to Day 5). At 6 h after Day 2 administration of IMQ, back-skin samples were collected for qRT-PCR. For IL-17a or CXCR2 antagonist administration, KO mice were treated with intraperitoneal (i.p.) injection of IL-17a antibody (Ab) on Day 0 or the CXCR2 antagonist every day from Days 0 to 5.
(**b**) IMQ-induced psoriasiform skin lesions and prevention trials using IL-17a Ab or CXCR2 antagonist: Clinical features and histopathology of the back skin on Day 6. WT or *Il36rn*$^{-/-}$ mice were administered IMQ for 5

days. For the prevention experiments, *Il36rn*$^{-/-}$ mice were treated with the IL-17a antibody (Ab), the CXCR2 antagonist, and a control Ab. Both clinically and histopathologically, the skin lesions of PV, but not of GPP, were reproduced in IMQ-treated *Il36rn*$^{-/-}$ mice (left column, bottom row). Administration of the IL-17a antibody or the CXCR2 antagonist attenuated the IMQ-induced PV skin lesions in the *Il36rn*$^{-/-}$ mice. Scale bar: 50 μm.

(**c**) Trans-epidermal water loss (TEWL) of IMQ-induced psoriasiform skin lesions and prevention trials. TEWL was measured in the back skin of WT or *Il36rn*$^{-/-}$ mice treated with IMQ (n= 4 mice), and prevention experiments were performed using the IL-17a antibody (n= 4 mice) or the CXCR2 antagonist (n= 4 mice). The IL-17a antibody significantly reduced TEWL in the IMQ-induced PV lesions in *Il36rn*$^{-/-}$ mice. Error bars represent mean±SD. *$p < 0.05$, data analyzed by unpaired one-way *t* test.

(**d**) Cytokine mRNA expression levels in IMQ-induced skin lesions. mRNA expression of cytokines implicated in psoriasiform skin inflammation were examined by qRT-PCR on WT or *Il36rn*$^{-/-}$ mice treated with IMQ (n= 4 mice). mRNA expression of *Il1b*, *Cxcl1* and *Il17a* significantly increased in IMQ-induced skin lesions of *Il36rn*$^{-/-}$ mice. Administration of each of the IL-17a antibody (n= 4 mice) and the CXCR2 (n= 4 mice) antagonist significantly attenuated the increase of *Il1b*, *Cxcl1* and *Il17a* mRNA expression. Error bars represent mean±SD.

Figure 3 Establishment and prevention of LPS-induced DITRA skin lesions in *Il36rn*$^{-/-}$ mice

(**a**) Protocols for the development of LPS-induced skin and liver lesions of DITRA. For the prevention experiments, mice were treated with intraperitoneal (i.p.) injection of TAK-242 or CXCR2 antagonist from Day

0 to Day 2 or with i.p. injection of IL-17a or control antibody (Ab) on Day 0.

(**b**) Clinical features of the back of the mice, H&E staining, immunohistochemistry (IHC) for TLR4 and macrophages (F4-80) of skin samples from the back on Day 3. The LPS-treated *Il36rn*$^{-/-}$ mouse shows erythema and abscesses (arrow). Histopathologically, intense neutrophilic infiltration is seen in the skin lesion (yellow circle). TLR4 expression is enhanced in the LPS-induced skin lesion in an *Il36rn*$^{-/-}$ mouse. Macrophage infiltration is apparent in the skin of both the LPS-treated WT mouse and the LPS-treated *Il36rn*$^{-/-}$ mouse. LPS-treated *Il36rn*$^{-/-}$ mice administered with TAK-242 do not present skin abscesses (left column, bottom row). TLR4 expression is markedly less intense in the LPS-treated *Il36rn*$^{-/-}$ mice administered with TAK-242 than in the LPS-treated *Il36rn*$^{-/-}$ mice, although macrophage infiltration is seen in the dermis of the LPS-treated *Il36rn*$^{-/-}$ mice administered with TAK-242. Scale bars: 200 μm (H&E staining) and 100 μm (IHC).

(**c**) The severity indices of skin lesions on Day 3 are significantly greater in the LPS-treated *Il36rn*$^{-/-}$ mice (n=14) than in the LPS-treated WT mice (n=16). Abscess formation is significantly attenuated in the LPS-treated *Il36rn*$^{-/-}$ mice administered with TAK-242 (n=8).

(**d**) Trials using anti-IL-17a antibody and CXCR2 antagonist were not successful in preventing LPS-induced DITRA-related skin lesions.

(**e**) *Cxcl1* and *Il6* mRNA expression levels in the back skin on Day 2 of LPS-treated *Il36rn*$^{-/-}$ mice (n=5) are significantly elevated compared with those in LPS-treated WT mice (n=6) and LPS-treated *Il36rn*$^{-/-}$ mice administered with TAK-242 (n=5).

(**f**) Concentrations of CXCL1, CXCL13 and IL-1β, but not IL-17a, are

significantly more elevated in the back skin of LPS-treated *Il36rn*$^{-/-}$ (KO) mice (n=4) than in LPS-treated wild-type (WT) mice (n=4) and in LPS-treated *Il36rn*$^{-/-}$ mice administered with TAK-242 (TAK) (n=4). Error bars represent mean±SD. ***P<0.001, **P<0.01, *P<0.05, data analyzed by unpaired one-way *t*-test.

Figure 4 Establishment and prevention of LPS-induced DITRA liver lesions in *Il36rn*$^{-/-}$ mice

(**a**) Naked-eye views (left column), histopathology (H&E staining) (central column) and IHC for macrophage infiltration (left column) of the liver from LPS- or DW-administered mice on Day 3, the day after the last LPS administration. Indurated nodules (right column, second row from bottom, arrow) are present, and histopathologically, abscesses (central column, second row from bottom, yellow circle) are apparent in the liver of the LPS-treated *Il36rn*$^{-/-}$ mouse. LPS-treated *Il36rn*$^{-/-}$ mice administered with TAK-242 show no nodules or abscesses in the liver. A palisading arrangement of macrophages is observed in the LPS-treated *Il36rn*$^{-/-}$ mouse (right column, second row from bottom, yellow arrows), but not in the LPS-treated WT mouse (right column, middle row) or in the LPS-treated *Il36rn*$^{-/-}$ mouse administered with TAK-242 (right column, bottom row). Scale bars: 100 μm.

(**b**) The frequency of liver abscesses in the LPS-treated mice was calculated on Day 3, the day after the last LPS application. The frequency of liver abscesses is significantly higher in the LPS-treated *Il36rn*$^{-/-}$ mice (n=14 mice) than in the LPS-treated WT mice (n=12 mice) and in the LPS-treated *Il36rn*$^{-/-}$ mice administered with TAK-242 (n=8 mice).

(**c**) Administration of anti-IL-17a Ab or CXCR2 antagonist does not

attenuate liver abscesses in the LPS-treated *Il36rn*$^{-/-}$ mice.

(**d**) Cytokine mRNA expression levels in the livers of LPS-treated DITRA mice. mRNA expression levels of cytokines in the liver were measured by qRT-PCR at Day 3 or Day 2 (4 h after the last LPS application) in DW- or LPS-treated WT mice (Day 3, n=4 mice and Day 2, n=5 mice), DW- or LPS-treated *Il36rn*$^{-/-}$ mice (Day 3, n=4 mice and Day 2, n=6 mice) and LPS-treated *Il36rn*$^{-/-}$ mice administered with TAK-242 (Day 3, n=4 mice and Day 2, n=5 mice). *Cxcl1* mRNA expression levels in the liver on Day 3 of LPS-treated *Il36rn*$^{-/-}$ mice are significantly elevated compared with those in LPS-treated WT mice. mRNA expression levels of *Cxcl1* (Day 3), *Il6* (Day 2), *Il1b* (Day 2) and *Tnf* (Day 3) in LPS-treated *Il36rn*$^{-/-}$ mice administered with TAK-242 are significantly lower compared with those in the livers of LPS-treated *Il36rn*$^{-/-}$ mice. ***P<0.001, *P<0.05, data analyzed by unpaired one-way *t*-test.

Figure 5 Lymph node cell subsets in an LPS-induced DITRA model in *Il36rn*$^{-/-}$ mice

Inguinal lymph node cells of WT or *Il36rn*$^{-/-}$ mice administrated with DW or LPS were stained with (**a**) CD3 and CD19, (**b**) CD3 and TCRγδ, (**c**) Gr-1 and CD11b, (**d**) Siglec-F and CD11c, and (**e**) α-GarCer/CD1d and TCRβ. B cells ($CD19^+CD3^-$) were significantly increased in LPS-treated *Il36rn*$^{-/-}$ mice (top left corner panel, red circle) compared with those in control non-LPS-treated WT and *Il36rn*$^{-/-}$ mice, and LPS-treated WT mice (**a**). **P<0.01, data analyzed by unpaired one-way *t*-test.

Figure 6 Establishment and prevention of LPS-induced DITRA enthesitis in *Il36rn*$^{-/-}$ mice

(**a**) Spontaneous enthesitis (white arrows) is observed in *Il36rn*$^{+/-}$ and *Il36rn*$^{-/-}$ mice, possibly induced by continual insult and minor injuries, but it is not observed in a wild-type (WT) mouse.

(**b**) Protocols for the development of LPS-induced enthesitis lesions of DITRA. For prevention by TAK-242, WT and *Il36rn*$^{-/-}$ mice were treated with intraperitoneal (i.p.) injection of TAK242 from Day 0 to 3.

(**c**) Clinical features and histopathology of the hind paw of the mice on Day 3, at 6 hours after the last LPS application. The hind paw of the LPS-treated *Il36rn*$^{-/-}$ mouse (left column, second bottom row) is swollen significantly compared with the hind paw of LPS-treated WT mice and LPS-treated *Il36rn*$^{-/-}$ mice administered TAK-242. Histopathologically, the LPS-treated *Il36rn*$^{-/-}$ mice exhibit neutrophilic infiltration around the metatarsophalangeal joint (arrow). No apparent neutrophilic infiltration is seen in the LPS-treated WT mice nor in the LPS-treated *Il36rn*$^{-/-}$ mice administered with TAK-242. B: bone. Scale bars: 100 μm.

(**d**) The increase in hind paw thickness in the LPS-treated *Il36rn*$^{-/-}$ mice (n=8 mice, 16 hind paws) is significantly greater than that in the LPS-treated WT mice (n=10 mice, 20 hind paws) and than that in the LPS-treated *Il36rn*$^{-/-}$ mice administered with TAK-242 (n=4 mice, 8 hind paws).

(**e**) Cytokine mRNA expression levels in LPS-treated hind paws with or without TAK-242 administration. mRNA expression levels of *Cxcl1*, *Il1b*, *Il6* and *Tnf* in the hind paw on Day 3 of LPS-treated *Il36rn*$^{-/-}$ mice (n=8) are elevated, but no significant difference is observed between LPS-treated *Il36rn*$^{-/-}$ mice and LPS-treated WT mice (n=7). However, the increase of *Cxcl1*, *Il1b*, *Il6* and *Tnf* mRNA expression is attenuated significantly in LPS-treated *Il36rn*$^{-/-}$ mice administered with TAK-242 (n=4).

Error bars represent mean±S.D. Data were analyzed by χ^2 test in (d) and by

unpaired one-way *t*-test in (e). ***$P<0.001$, *$P<0.05$.

a

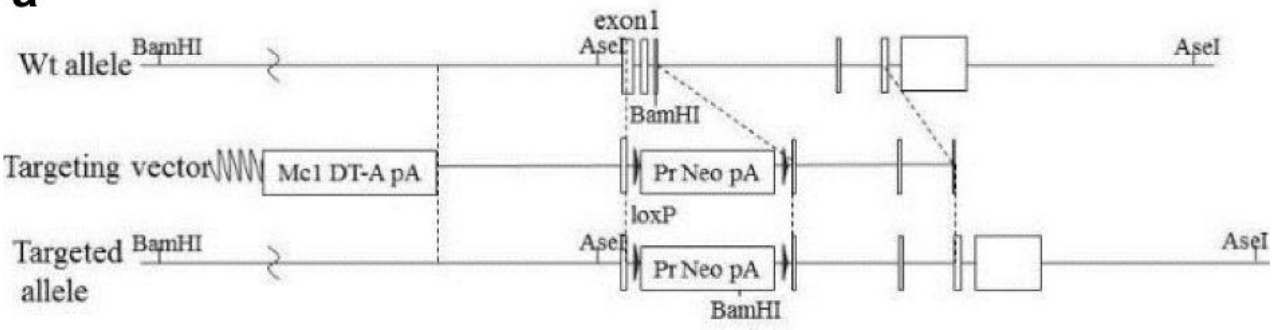

b

293-bp mutant band

205-bp WT band

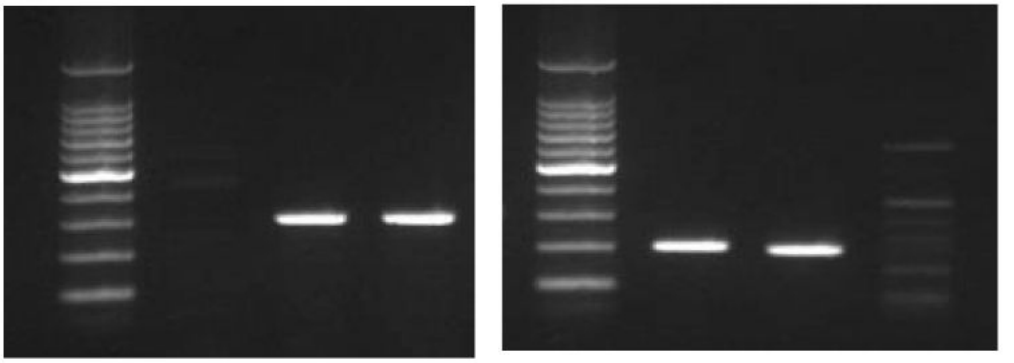

WT

Il36rn$^{+/-}$

Il36rn$^{-/-}$

WT

Il36rn$^{+/-}$

Il36rn$^{-/-}$

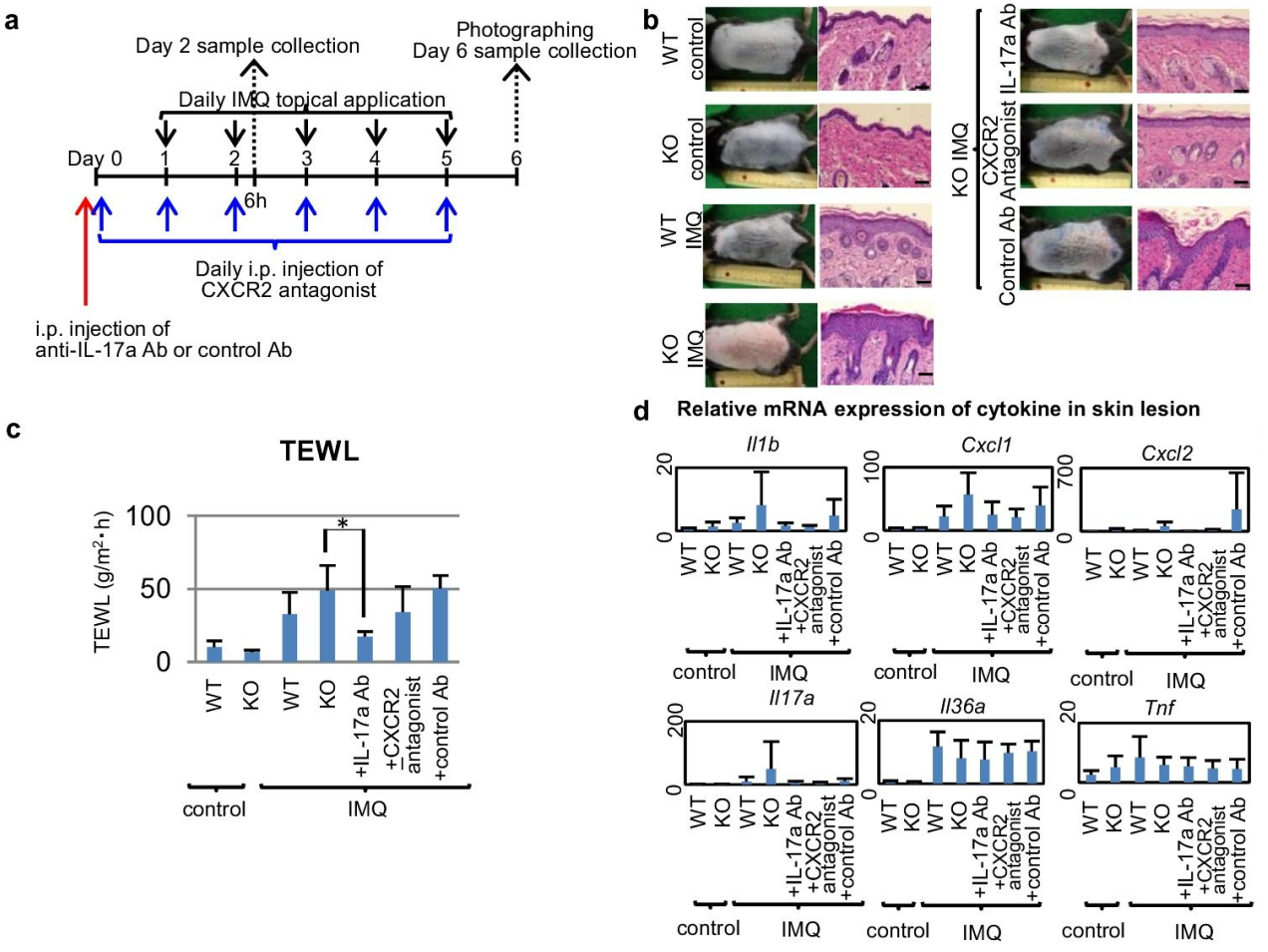
a
Day 2 sample collection
Photographing
Day 6 sample collection
Daily IMQ topical application
Day 0
1
2
3
4
5
6
6h
Daily i.p. injection of
CXCR2 antagonist
i.p. injection of
anti-IL-17a Ab or control Ab
b
WT control
KO control
WT IMQ
KO IMQ
KO IMQ
IL-17a Ab
CXCR2 Antagonist
Control Ab
c
TEWL
TEWL (g/m²・h)
100
50
0
*
WT
KO
WT
KO
+IL-17a Ab
+CXCR2 antagonist
+control Ab
control
IMQ
d
Relative mRNA expression of cytokine in skin lesion
Il1b
Cxcl1
Cxcl2
Il17a
Il36a
Tnf
20
100
700
200
0
WT
KO
+IL-17a Ab
+CXCR2 antagonist
+control Ab
control
IMQ

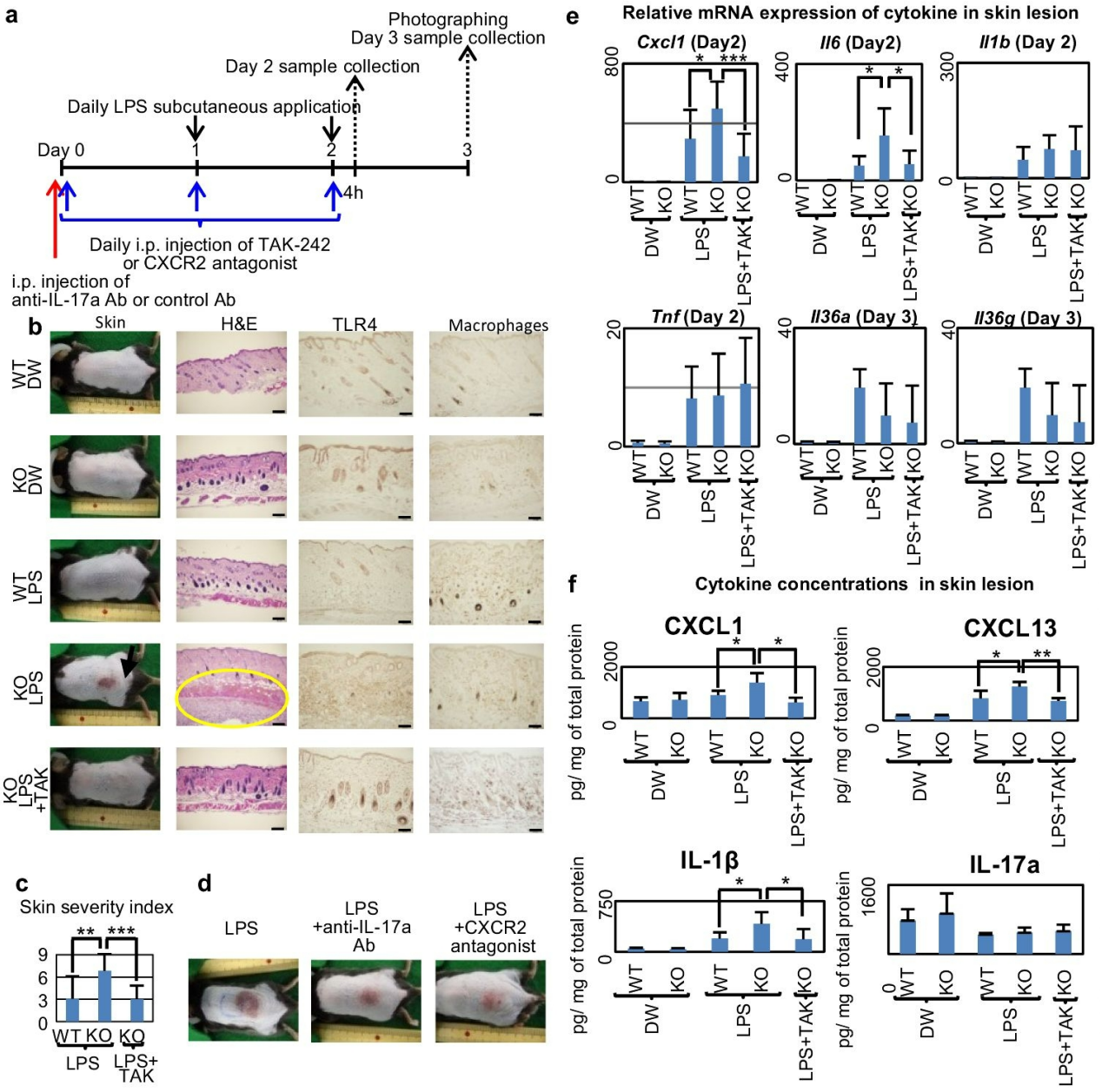
a
Photographing
Day 3 sample collection
Day 2 sample collection
Daily LPS subcutaneous application
Day 0
1
2
3
4h
Daily i.p. injection of TAK-242
or CXCR2 antagonist
i.p. injection of
anti-IL-17a Ab or control Ab
b
Skin
H&E
TLR4
Macrophages
WT DW
KO DW
WT LPS
KO LPS
KO LPS +TAK
c
Skin severity index
WT KO KO
LPS
LPS+ TAK
d
LPS
LPS +anti-IL-17a Ab
LPS +CXCR2 antagonist
e
Relative mRNA expression of cytokine in skin lesion
Cxcl1 (Day2)
Il6 (Day2)
Il1b (Day 2)
Tnf (Day 2)
Il36a (Day 3)
Il36g (Day 3)
WT KO
DW
LPS
LPS+TAK
f
Cytokine concentrations in skin lesion
CXCL1
CXCL13
IL-1β
IL-17a
pg/ mg of total protein

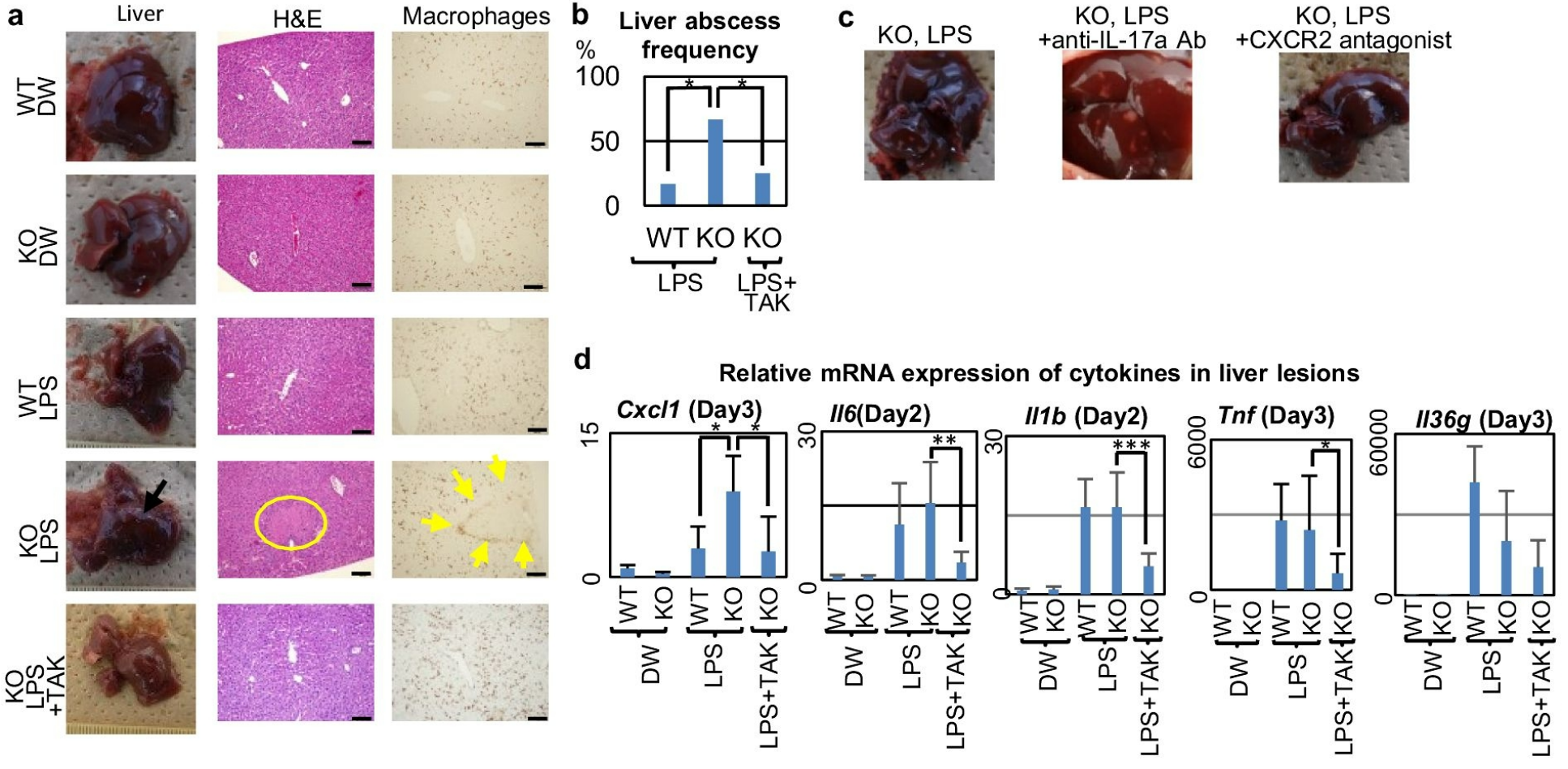
a
Liver
H&E
Macrophages
WT DW
KO DW
WT LPS
KO LPS
KO LPS +TAK
b
Liver abscess frequency
%
100
50
0
WT KO KO
LPS
LPS+ TAK
c
KO, LPS
KO, LPS +anti-IL-17a Ab
KO, LPS +CXCR2 antagonist
d
Relative mRNA expression of cytokines in liver lesions
Cxcl1 (Day3)
Il6(Day2)
Il1b (Day2)
Tnf (Day3)
Il36g (Day3)
WT KO WT KO KO
DW
LPS
LPS+TAK

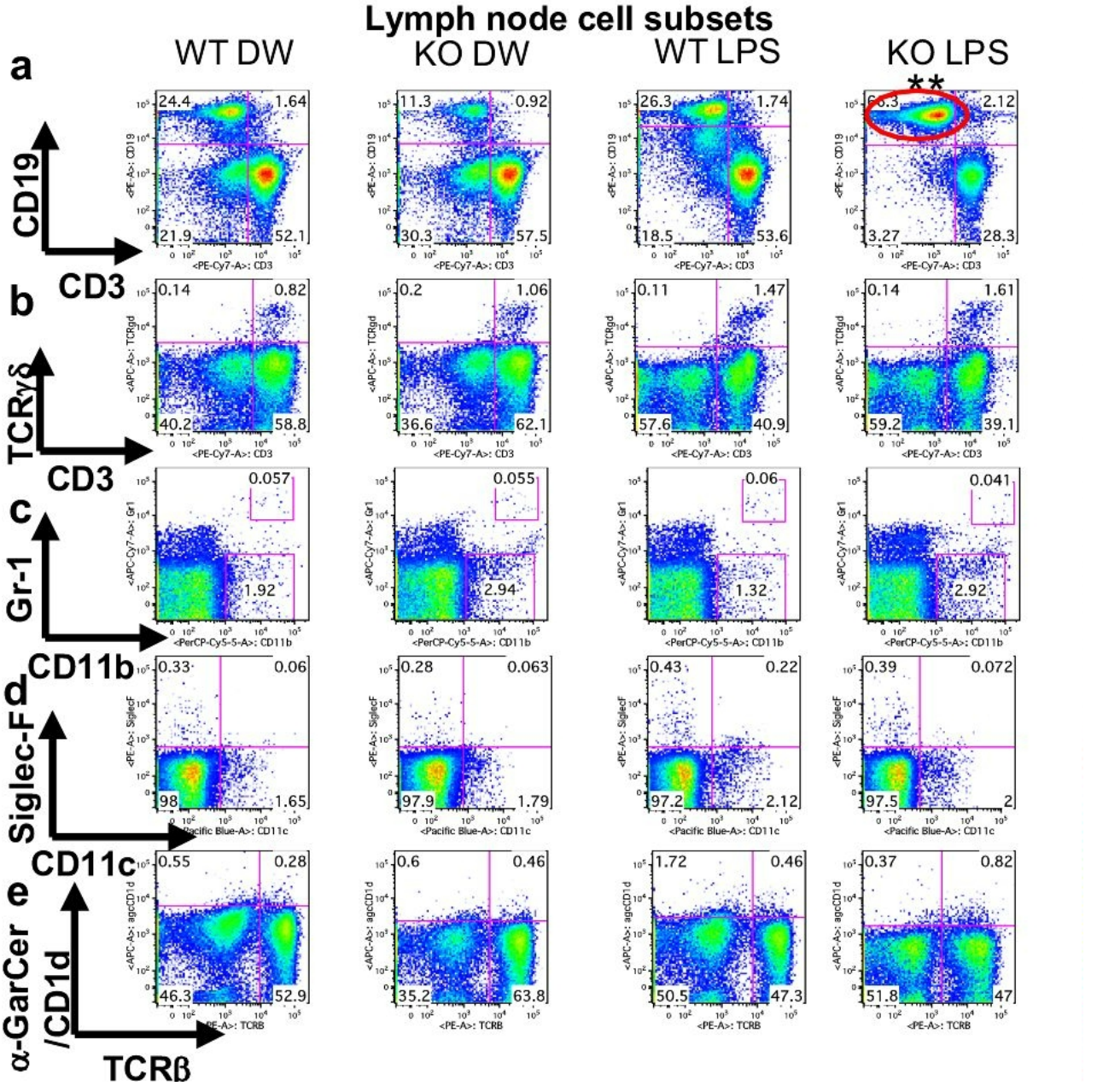
Lymph node cell subsets
WT DW
KO DW
WT LPS
KO LPS
**
a
CD19
CD3
24.4
1.64
21.9
52.1
11.3
0.92
30.3
57.5
26.3
1.74
18.5
53.6
66.3
2.12
3.27
28.3
b
TCRγδ
CD3
0.14
0.82
40.2
58.8
0.2
1.06
36.6
62.1
0.11
1.47
57.6
40.9
0.14
1.61
59.2
39.1
c
Gr-1
CD11b
0.057
1.92
0.055
2.94
0.06
1.32
0.041
2.92
d
Siglec-F
CD11c
0.33
0.06
98
1.65
0.28
0.063
97.9
1.79
0.43
0.22
97.2
2.12
0.39
0.072
97.5
2
e
α-GarCer /CD1d
TCRβ
0.55
0.28
46.3
52.9
0.6
0.46
35.2
63.8
1.72
0.46
50.5
47.3
0.37
0.82
51.8
47

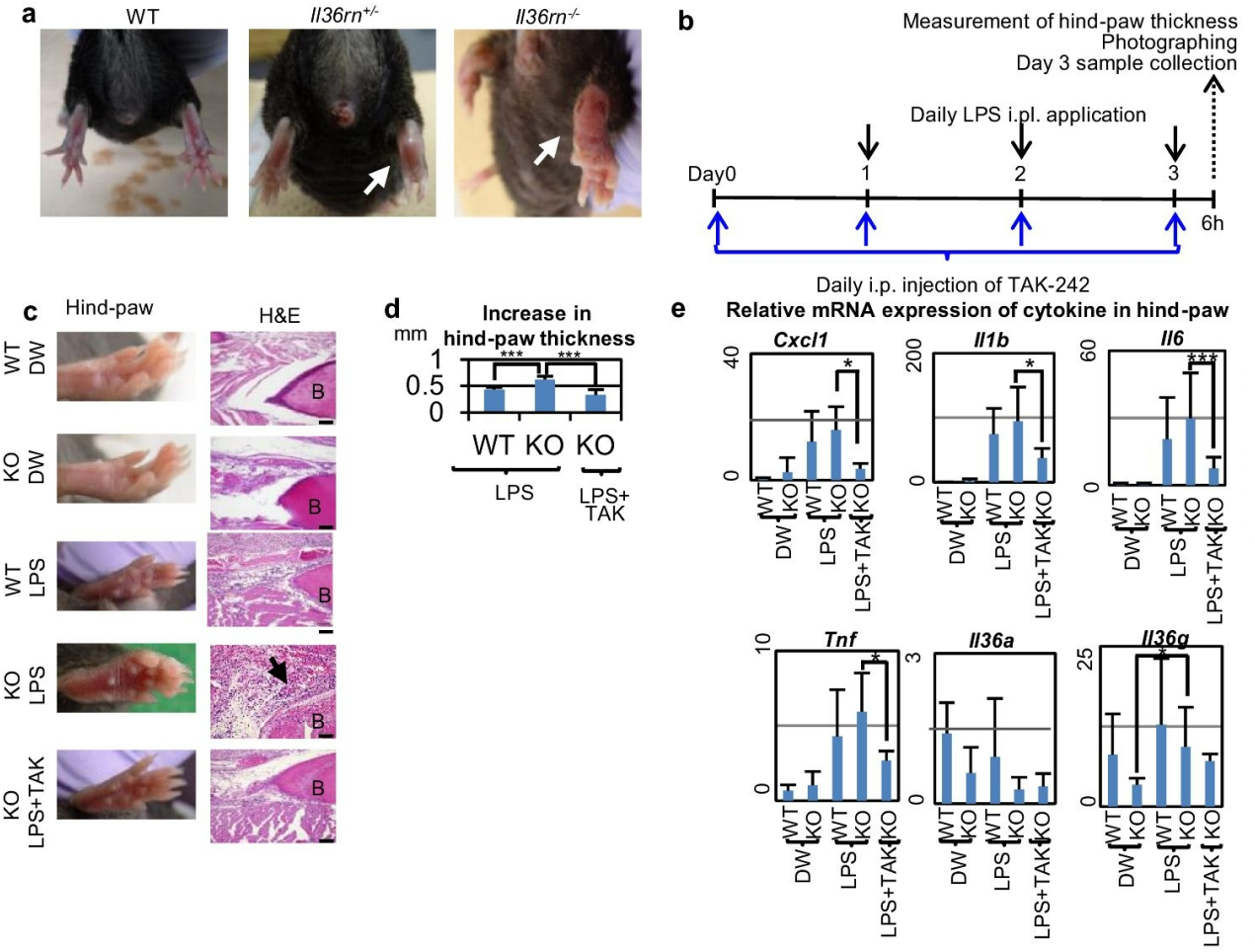
a
WT
Il36rn+/-
Il36rn-/-
b
Measurement of hind-paw thickness
Photographing
Day 3 sample collection
Daily LPS i.pl. application
Day0
1
2
3
6h
Daily i.p. injection of TAK-242
c
Hind-paw
H&E
WT DW
KO DW
WT LPS
KO LPS
KO LPS+TAK
B
d
Increase in hind-paw thickness
mm
1
0.5
0
***
***
WT KO KO
LPS
LPS+ TAK
e
Relative mRNA expression of cytokine in hind-paw
Cxcl1
Il1b
Il6
Tnf
Il36a
Il36g
WT KO WT KO KO
DW
LPS
LPS+TAK

Highlights

- Deficiency of IL-36 receptor antagonist (DITRA) model mice was established.
- The involvement of TLR4 signaling in the pathogenesis of DITRA was clearly demonstrated.
- Blockage of TLR4 signaling was shown as a promising treatment for DITRA.

Supplementary Table 1. Nucleotide sequences of primers and probes used for qRT-PCR

Il1b NM_008361	Forward Primer	CCTGATGAGAGCATCCAG
	Reverse Primer	GAGGATGGGCTCTTCTTC
	Probe	AATCTCGCAGCAGCACATCAAC
Il6 NM_031168	Forward Primer	GCCTTCTTGGGACTGATG
	Reverse Primer	GTGGTATAGACAGGTCTGTTG
	Probe	TGGTATCCTCTGTGAAGTCTCCTCT
Il17a NM_010552	Forward Primer	GAGCTTCATCTGTGTCTC
	Reverse Primer	GACCTTCACATTCTGGAG
	Probe	CTGTTGCTGCTGCTGAGCCT
Tnf NM_013693	Forward Primer	GGATGAGAAGTTCCCAAA
	Reverse Primer	ACTCGAATTTTGAGAAGATG
	Probe	CCTCCCTCTCATCAGTTCTATGGC
Il36a (Il1f6) NM_019450	Forward Primer	CAGTCCCAAGGAAAGAG
	Reverse Primer	CCTGTTCGTCTCAAGAG
	Probe	AGTTCCAGTCACTATTACCTTGCTCC
Il36b (Il1f8) NM_027163	Forward Primer	CTGACTGGAAATACTTTAACA
	Reverse Primer	GTGTCTCTACATGCTATCA
	Probe	CTAGCAACAATGTCAAGCCTGTCAT
Il36g (Il1f9) NM_153511	Forward Primer	GTGGATCTTTCGTAATCAG
	Reverse Primer	TCCCAAATAAATGGCAATC
	Probe	ACAGTTCCACGAAGCCACAGA
Cxcl1 NM_008176	Forward Primer	CCTCAAGAACATCCAGAG
	Reverse Primer	GGACAATTTTCTGAACCAA
	Probe	CTTCAGGGTCAAGGCAAGCCTC
Cxcl2 NM_009140	Forward Primer	CTGTCAATGCCTGAAGAC
	Reverse Primer	GAGTGGCTATGACTTCTG
	Probe	TTGACTTCAAGAACATCCAGAGCTT
Gapdh NM_008084	Forward Primer	CCCACTAACATCAAATGG
	Reverse Primer	CATGGTGGTGAAGACA
	Probe	AGACTCCACGACATACTCAGCAC

a Skin erythema areas

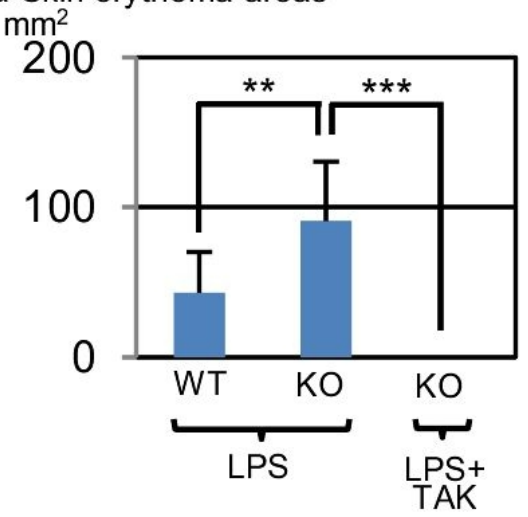

b Skin abscess/edema areas

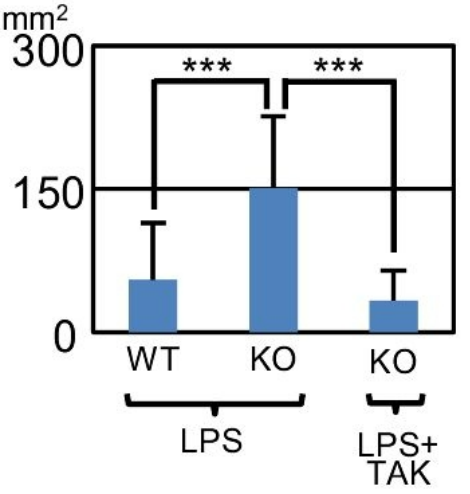

c Skin erythema severity score

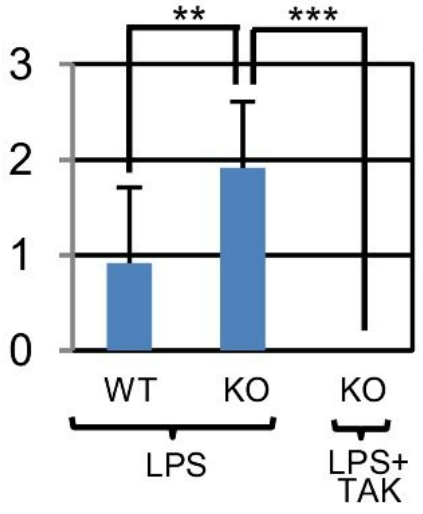

d Skin abscess/edema severity score

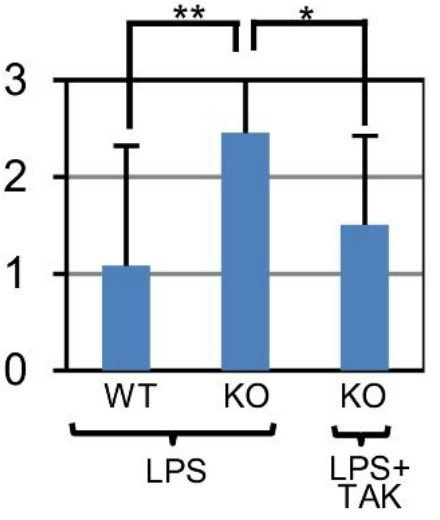

Supplementary Figure legends

Figure S1 Quantitative analysis of LPS-induced DITRA skin lesions in *Il36rn*$^{-/-}$ mice

(a, b) The areas of skin lesions (erythema (a) and abscess/edema (b)) on Day 3 are significantly greater in the LPS-treated *Il36rn*$^{-/-}$ mice (n=14) than in the LPS-treated WT mice (n=16). The formation of erythema (a) and abscess/edema (c) is significantly attenuated in the LPS-treated *Il36rn*$^{-/-}$ mice administered with TAK-242 (n=8).

(c, d) The area scores of skin erythema (c) and abscess/edema (d) on Day 3 are also significantly greater in the LPS-treated *Il36rn*$^{-/-}$ mice than in the LPS-treated WT mice. The area scores of erythema (c) and abscess/edema (d) are significantly reduced in the LPS-treated *Il36rn*$^{-/-}$ mice administered with TAK-242. Error bars represent mean±SD. ***$P<0.001$, **$P<0.01$, *$P<0.05$, data analyzed by unpaired one-way *t*-test."